

## High-pressure phase transition in titanite (CaTiOSiO<sub>4</sub>)

MARTIN KUNZ,<sup>1</sup> DIMITRIOS XIROUCHAKIS,<sup>2</sup> DONALD H. LINDSLEY,<sup>2</sup> AND DANIEL HÄUSERMANN<sup>1</sup>

<sup>1</sup>High Pressure Group, European Synchrotron Radiation Facility, F-38043 Grenoble, France

<sup>2</sup>Center for High Pressure Research and Department of Earth and Space Sciences, State University of New York at Stony Brook, Stony Brook, New York 11794, U.S.A.

### ABSTRACT

A pressure-induced phase transition was observed in a sample of synthetic titanite (CaTiOSiO<sub>4</sub>). The high-pressure structure was refined in space group *A2/a* [ $a = 6.8912(3)$ ,  $b = 8.6234(3)$ ,  $c = 6.4065(3)$  Å,  $\beta = 113.057(4)^\circ$ ] using powder diffraction data collected with synchrotron radiation on material in a diamond-anvil cell at 69.5 kbar. The observed  $P2_1/a \leftrightarrow A2/a$  symmetry change is identical to the well-described phase change at 496 K. However, the mechanism of the phase transition is proposed to be different. The high-temperature phase transition is assumed to result from a loss of long-range order between Ti off-center dipoles, while locally preserving the characteristic off-center displacement of Ti atoms. In contrast, the high-pressure phase transition is a response to increasing overbonding of the Ti atoms, which forces individual Ti atoms to shift to the center of the coordination octahedron. Thus, the *A2/a* high-pressure phase, unlike the *A2/a* high-temperature phase, has both local and long-range *A2/a* symmetry.

### INTRODUCTION

The structure of titanite (CaTiOSiO<sub>4</sub>) is characterized by corner-linked chains of TiO<sub>6</sub> octahedra parallel to [100], interlaced with edge-sharing chains of CaO<sub>7</sub> polyhedra parallel to [101]. Unpolymerized SiO<sub>4</sub> tetrahedra share corners with both structural units (Speer and Gibbs 1976; Taylor and Brown 1976; Ghose et al. 1991). As is very typical for octahedrally coordinated Ti<sup>4+</sup>, the Ti atoms in the *P2<sub>1</sub>/a* ambient-condition phase are located in off-center positions within the TiO<sub>6</sub> octahedra. The orientations of the off-center dipole vectors are subparallel within an individual TiO<sub>6</sub> chain but in opposite directions between neighboring chains.

The titanite structure undergoes a phase transition at 496 K and ambient pressure. This phase transition has been thoroughly investigated (Speer and Gibbs 1976; Ghose et al. 1991; Higgins and Ribbe 1976; Oberti et al. 1991; Taylor and Brown 1976; Bismayer et al. 1992; Zhang et al. 1995). The high-*T* phase transition at 496 K is mainly affected by a change in the position of the Ti<sup>4+</sup> cations within the O octahedron. The off-center position of the Ti atom at ambient conditions lowers the *A2/a* symmetry of the high-*T* phase to *P2<sub>1</sub>/a*. At high temperature, no Ti off-center distortions can be resolved, and the average symmetry increases to space group *A2/a*. However, birefringence data, IR spectroscopy, dielectric response, heat-capacity measurements, and diffraction experiments all indicate that the observed *A2/a* symmetry above 496 K results from a loss of long-range coherence between individual Ti off-center dipoles rather than true *A2/a* symmetry (Zhang et al. 1995; Bismayer et al. 1992). Zhang et al. (1995) suggested that a second possible

phase anomaly at about 800 K may be the transition to true *A2/a* symmetry, in which the off-center dipole vanishes within the individual TiO<sub>6</sub> octahedra.

As shown by Kunz and Brown (1995), this kind of off-center distortion is typical for octahedrally coordinated d<sup>0</sup> transition metals. In the case of Ti<sup>4+</sup>, its occurrence is strongly dependent on an interplay between structural forces and intrinsic electronic effects, and thus Ti<sup>4+</sup>, unlike V<sup>5+</sup> or Mo<sup>6+</sup>, is found in distorted as well as undistorted coordination, depending on the structural topology. Their model predicts that in phases that contain distorted TiO<sub>6</sub> octahedra, such as titanite, the out-of-center distortion of the Ti<sup>4+</sup> cations can be removed by structural manipulation, such as chemical substitution or changes in intensive variables like pressure and temperature. Furthermore, the distortion theorem (e.g., Brown 1992) states that the bond-valence sum is smaller for a coordination arrangement with equal bond lengths than for a polyhedron in which individual bonds deviate from the average value. The implication is that the application of high pressure on a crystal structure, which leads to overbonding of the individual atoms because of structural compression, is very likely to remove coordination distortions or even to increase the coordination number (e.g., Kunz et al. 1996).

With the use of synchrotron powder diffraction data, we show in this paper that this behavior is observed in titanite (CaTiOSiO<sub>4</sub>) at high pressures.

### EXPERIMENTAL PROCEDURES

#### Sample synthesis and characterization

The titanite sample was synthesized in subsolidus conditions by reacting an equimolar mixture of dry CaSiO<sub>3</sub>

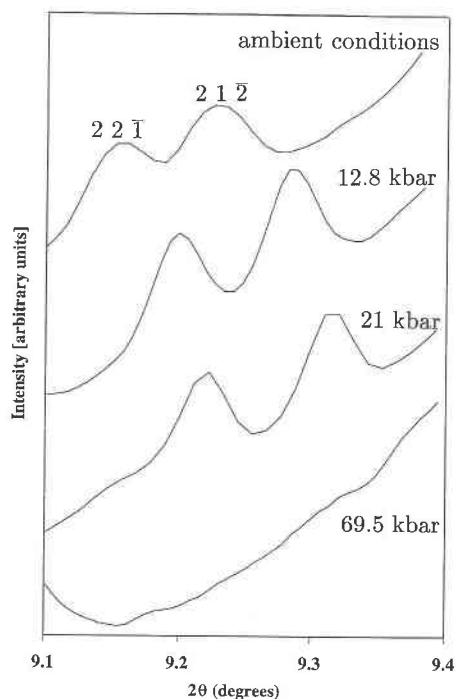


FIGURE 1. Evolution of  $2\bar{2}\bar{1}$  and  $2\bar{1}\bar{2}$  reflections with pressure. The slope in the background is due to the 031 reflection at  $9.65^\circ 2\theta$ .

and  $\text{TiO}_2$  in a platinum crucible at  $1100^\circ\text{C}$  for 14 d and  $1200^\circ\text{C}$  for 21 d with repeated cycles of thorough grinding (2–3 h) during annealing. Optical examination during electron microprobe analysis revealed the presence of several (three to five) grains of  $\text{CaSiO}_3$  and one grain of  $\text{SiO}_2$  as cores in titanite grains. The presence of small amounts of either  $\text{CaSiO}_3$  or  $\text{SiO}_2$  is also suggested by the presence of a weak and somewhat broad nontitanite peak at about  $4.1 \text{ \AA}$  (i.e., 110 of low quartz or  $\bar{1}\bar{1}0$  of wollastonite) in the diffraction data.

The  $\text{CaSiO}_3$  was synthesized from a mechanical mixture of  $\text{CaCO}_3$  (ALPHA lot 050980) and  $\text{SiO}_2$  (JM S50389B). These powders were dried at  $400^\circ\text{C}$  (4 h) and  $1000^\circ\text{C}$  (30 h), respectively, before weighing. Subsequently, the  $\text{CaCO}_3$ - $\text{SiO}_2$  mixture was ground in ethanol in an automatic agate mortar for 3 h. The mixture was slowly decarbonated over a period of 24–30 h (from  $500$  to  $1000^\circ\text{C}$ ) and then reacted at  $1100^\circ\text{C}$ . During annealing, it was ground several times until optical examination and powder X-ray diffraction suggested that only wollastonite was present. The final product was stored in a desiccator. Before weighing,  $\text{CaSiO}_3$  and  $\text{TiO}_2$  were dried at  $1100^\circ\text{C}$  for 5 and 30 h, respectively, and  $\text{SiO}_2$  at  $1000^\circ\text{C}$  for 30 h.

The sample was chemically analyzed for Ca, Ti, Si, and O using a four-spectrometer Cameca CAMEBAX electron microprobe. The measured composition corresponds within the experimental uncertainty to ideal titanite.

TABLE 1. Cell parameters and structure refinement details of the X-ray diffraction experiment

	12.5 kbar	21 kbar	69.5 kbar
$a(\text{\AA})$	7.02631(9)	7.00023(7)	6.8912(3)
$b(\text{\AA})$	8.6930(1)	8.6813(1)	8.6234(4)
$c(\text{\AA})$	6.5216(1)	6.50408(8)	6.4065(3)
$\beta(^{\circ})$	113.644(1)	113.560(1)	113.057(4)
No. of reffs.			187
$R_p$ (%)			1.04
$R_{wp}$ (%)			1.88
$R_{\text{res}}$ (%)			7.40
$(\sin\theta)/\lambda_{\text{max}}$			0.50
$\lambda(\text{\AA})$			0.4350(1)
Space group			$A2/a$
Abs. corr.			no
Soft constr.			Si-O = $1.63 \text{ \AA}$

### X-ray diffraction

The sample was manually ground in an agate mortar under ethanol. The fraction still in suspension after settling for 2 min was loaded into a Chervin-type diamond-anvil cell with  $600 \mu\text{m}$  culet diamonds. The sample was loosely packed into a  $180 \mu\text{m}$  hole within a steel gasket together with a 1:4 mixture of methanol:ethanol used as the pressure medium. The diamond-anvil cell was centered in an X-ray beam of wavelength  $0.4350(1) \text{ \AA}$  ( $28.4 \text{ keV}$ ), selected from an undulator beam of beamline ID30 at the European Synchrotron Radiation Facility (ESRF) using a channel-cut Si(111) monochromator. The wavelength and detector-to-sample distance were calibrated using an Si standard (NBS 640). Data were collected at 0, 12.5, 21, and 69.5 kbar (ruby fluorescence pressure calibration; Hazen and Finger 1982) and recorded on a Fuji image plate, which was read on a Molecular Dynamics Phosphor2 image-plate reader. Raw data were corrected for image-plate reader-induced distortion using a calibration-grid exposure before correcting for the tilt of the image plate relative to the incident beam. The corrected two-dimensional pattern was integrated into a one-dimensional  $2\theta$ -vs.-intensity array, which was used for subsequent structural (Rietveld) analysis. All two-dimensional analysis up to the integration was performed using the program Fit2d (Hammersley 1996).

Integrated data were further processed using the program GSAS (Larson and Von Dreele 1986). In the first stage, the patterns were scrutinized for possible isolated reflections of the type  $hkl$ ,  $k + l = \text{odd}$ . This was necessary because the difference between  $P2_1/a$  and  $A2/a$  symmetry is very subtle, and in titanite it is revealed only by the additional presence of very weak reflections of this type in  $P2_1/a$ . Because of strong overlaps in the low-symmetry powder diffraction pattern, none of the  $h0l$  reflections, which in  $P2_1/a$  titanite are the strongest reflections of the class  $hkl$ ,  $k + l = \text{odd}$ , could be used for this purpose. In fact only  $2\bar{2}\bar{1}$  ( $F^2 = 216$ ) and  $2\bar{1}\bar{2}$  ( $F^2 = 232$ ) are separated sufficiently to be used as unambiguous indicators of symmetry. A high X-ray flux as obtained from third-generation synchrotron sources is thus crucial for such an experiment to be successful in a diamond-anvil

**TABLE 2.** Atomic coordinates and displacement parameters of CaTiOSiO<sub>4</sub> at 69.5 kbar (space group *A2/a*)

	<i>x</i>	<i>y</i>	<i>z</i>	<i>U</i> <sub>iso</sub> (Å <sup>2</sup> )
Ca	¼	0.1666(6)	0	0.019(3)
Ti	½	0	½	0.016(2)
Si	¾	0.188(1)	0	0.014(3)
O1	¾	0.061(1)	½	0.011(4)*
O2	0.922(1)	0.0712(8)	0.179(1)	0.011(4)*
O3	0.392(1)	0.216(9)	0.391(1)	0.011(4)*

\* Displacement parameters for O were constrained to be equal.

cell. Because these reflections were not observed at 69.5 kbar (Fig. 1), space group *A2/a* was used in a subsequent LeBail fit (LeBail 1992) of this data set, where background parameters (shifted Chebyshev, 24 parameters), peak-profile parameters [multiterm Simpson's rule integration of pseudo Voigt (Howard 1982; Thompson et al. 1987)], and cell parameters were refined. After convergence, background and peak-profile parameters were fixed before switching to full-profile structure refinement, varying atomic coordinates and isotropic displacement parameters (*U*<sub>iso</sub>), where *U*<sub>iso</sub> values for O atoms were constrained to be equal. A soft constraint of 1.63 Å ( $\sigma = 0.005$  Å, weight = 10) was initially applied to the Si-O bond lengths to prevent divergence of the refinement. In the final stages of the refinement, background and peak-profile parameters were varied together with the structural parameters, at which time the soft constraints were abandoned. Further experimental details are given in Table 1.

## RESULTS AND DISCUSSION

Refined atomic positional coordinates are given in Table 2. Figure 1 shows the evolution of the 22 $\bar{1}$  and 21 $\bar{2}$  reflections, which were used as indicators to differentiate between space groups *P2<sub>1</sub>/a* and *A2/a*. Although very weak even at ambient conditions, 12.8 kbar, and 21 kbar, their disappearance at or below 69.5 kbar is clear and indicates that a phase transition to the higher symmetry (*A2/a*) phase occurs between 21 kbar and 69.5 kbar.

Table 3 compares some distance and bond-angle values at 1 bar and 69.5 kbar. The most important structural change due to compression is the disappearance of the characteristic out-of-center distortion of the Ti atom within its octahedral O surroundings. In contrast to the apparently identical phase transition at high temperature, where the observed disappearance of the out-of-center distortion is due to a loss of long-range order between individual off-center dipoles (e.g., Bismayer et al. 1992; Zhang et al. 1995), we believe this to be a real centering, i.e., the Ti atoms indeed move into the center of their coordination octahedra. This interpretation is based on crystal-chemical reasoning. The refined bond lengths for the high-pressure Ti octahedron (Table 3) translate into a bond-valence sum (e.g. Brown 1992) of 4.39 valence units (v.u.), which indicates significant overbonding. This is expected for a structure at high pressure. However, following the distortion theorem (e.g., Brown 1992) this Ti

**TABLE 3.** Selected interatomic distances (Å) and angles (°) for CaTiOSiO<sub>4</sub> at 69.5 kbar and ambient conditions

	69.5 kbar ( <i>A2/a</i> )	Ambient conditions ( <i>P2<sub>1</sub>/a</i> )*
Ca-O1	2.35(1)	2.284(4)
Ca-O2	2.421(8)	2.406(9)
Ca-O2	2.421(8)	2.405(9)
Ca-O3	2.346(8)	2.41(1)
Ca-O3	2.346(8)	2.674(9)
Ca-O3	2.499(9)	2.41(1)
Ca-O3	2.499(9)	2.584(9)
(Ca-O)	2.412	2.453
Ca bond-valence sum (v.u.)**	2.13	1.98
Ti-O1	1.801(3)	1.771(9)
Ti-O1	1.801(3)	1.970(9)
Ti-O2	2.010(7)	1.975(7)
Ti-O2	2.010(7)	2.038(9)
Ti-O3	2.027(7)	2.012(7)
Ti-O3	2.027(7)	2.012(9)
(Ti-O)	1.946	1.963
Ti bond-valence sum (v.u.)**	4.4	4.2
Ti-O1-Ti	146.1(6)	141.4(2)
Ca-O1-Ti	106.95(3)	110.8(3)
Ca-O1-Ti	106.95(3)	107.8(4)
Ca-O2-Ti	96.3(3)	99.2(2)
Ca-O2-Ti	96.3(3)	100.0(3)
Ca-O2-Si	95.9(5)	96.1(4)
Ti-O2-Si	137.3(3)	137.2(4)
Ca-O3-Ca	108.9(3)	109.6(3)
Ca-O3-Ti	98.2(3)	98.5(3)
Ca-O3-Ti	98.2(3)	99.2(2)

\* Data from Kunz et al. (1997).

\*\* As defined by Brown (1992).

bond-valence sum would be even higher if it were a distorted octahedron as it exists at ambient conditions. Assuming a typical off-center shift of 0.1 Å, a distorted octahedron at high pressure would yield a bond-valence sum of 4.47 v.u. The same effect can also be observed for the pivot O1 atom, which links the Ti metals along the octahedral chain and thus forms the distorted Ti-O bonds at ambient conditions. Here, a distorted arrangement at high pressure would increase its bond-valence sum from 2.44 to 2.52 v.u. The pressure-induced compressional stress on the Ti and O1 atoms can thus be partially relieved by positioning the Ti cation in the center of the octahedron, leading to an increase in symmetry from *P2<sub>1</sub>/a* to *A2/a*.

The high-*P* phase, like the high-*T* phase, is topologically identical to the *P2<sub>1</sub>/a* structure of titanite. The difference among these is mainly revealed in the subtle coordination change around the Ti cation. However, despite the identical symmetry, the high-*T* and high-*P* phases are not structurally equivalent because of their different local TiO<sub>6</sub> geometry. Because of this, it would be interesting to map the phase boundaries in *T-P* space between the high-*T* *A2/a* and high-*P* *A2/a* phases and also to investigate further the proposed phase transition at 800 K (Zhang et al. 1995) and its relation to the high-*P* phase. In anorthite (CaAl<sub>2</sub>Si<sub>2</sub>O<sub>8</sub>), in which a similar situation of identical symmetry change can be observed at high-*T* and high-*P*, such a study revealed an isosymmetric phase transition linking the high-*T* and high-*P* phases (Hackwell

and Angel 1995). It must be emphasized that our present interpretation of the titanite high-*P* structure is based on indirect crystal-chemical arguments, and the presence of both short- and long-range *A2/a* symmetry must be confirmed by another experimental technique.

Among the M-O polyhedra in titanite, the relatively weakly bonding CaO<sub>7</sub> polyhedron undergoes the most compression with increasing pressure. This is revealed by an average bond-length decrease of 1.7%. For the Ti octahedron, the strongest compression is along the O1-Ti-O1 diagonal, which is subparallel to the Ti-O-Ti chain and, at ambient conditions, also parallel to the off-center vector. This asymmetric compression of the TiO<sub>6</sub> octahedron is caused by the tight interlacing of the CaO<sub>7</sub> chains with the TiO<sub>6</sub> chains. The large shrinkage of the former induces large compression along [100] of the latter. In the directions perpendicular to the Ti-O-Ti axis, we observed a rigid behavior of the Ti octahedra. Most of the compression in these directions is accommodated by the CaO<sub>7</sub> polyhedra without any competing interference with other structural units.

At first glance, the relatively large increase of the Ti-O1-Ti pivot angle from 141.4° at ambient conditions to 146.1° at 69.5 kbar is surprising. However, this can be explained by the relatively large compression of the CaO<sub>7</sub> structural units. The CaO<sub>7</sub> polyhedra share edges with TiO<sub>6</sub> octahedra such that two neighboring Ti octahedra enclose a CaO<sub>7</sub> polyhedron on the opposite side of the 141° pivot angle. A relatively large compression of the CaO<sub>7</sub> polyhedra, therefore, opens this pivot angle more, thus straightening the TiO<sub>6</sub> chain. This straightening must be compensated by shrinkage of a Ti-O bond in this direction, as explained above. All other observed angles between structural units decrease in accordance with a compressional effect resulting from high pressure.

The above-described microscopic changes result in a volume decrease of 5.1% between ambient pressure and 69.5 kbar. The *a*, *b*, and *c* cell parameters decrease by 2.4, 1.0, and 2.3%, respectively, within the investigated pressure range. The relatively stiff behavior of the *b* axis agrees with our microscopic observation that the Ca polyhedra, which are polymerized along [101], show the largest volume decrease.

#### ACKNOWLEDGMENTS

D.H.L. and D.X. acknowledge support from NSF grant EAR-9304699. The help of Michael Hanfand on beamline ID30 is highly appreciated. Useful comments by J.A. Speer, J.M. Hughes, and an anonymous referee helped to improve the manuscript.

#### REFERENCES CITED

- Bismayer, U., Schmahl, W., Schmidt, C., and Groat, L.A. (1992) Linear birefringence and X-ray diffraction studies of the structural phase transition in titanite CaTiSiO<sub>5</sub>. *Physics and Chemistry of Minerals*, 19, 260–266.
- Brown, I.D. (1992) Chemical and steric constraints in inorganic solids. *Acta Crystallographica*, B48, 553–572.
- Ghose, S., Ito, Y., and Hatch, D.M. (1991) Paraelectric-antiferroelectric phase transition in titanite, CaTiSiO<sub>5</sub>: I. A high temperature X-ray diffraction study of the order parameter and transition mechanism. *Physics and Chemistry of Minerals*, 17, 591–603.
- Hackwell, T.P., and Angel, R.J. (1995) Reversed brackets for the  $P\bar{1} \rightleftharpoons \bar{1}I$  transition in anorthite at high pressures and temperatures. *American Mineralogist*, 80, 239–246.
- Hazen, R.M., and Finger, L.W. (1982) *Comparative crystal chemistry*, 231 p. Wiley, New York.
- Hammersley, A. (1996) Fit2d reference manual. European Synchrotron Radiation Facility, internal publication.
- Higgins, J.B., and Ribbe, P.H. (1976) The crystal chemistry and space groups of natural and synthetic titanites. *American Mineralogist*, 61, 878–888.
- Howard, C.J. (1982) The approximation of asymmetric neutron powder diffraction peaks by sums of gaussians. *Journal of Applied Crystallography*, 15, 615–620.
- Kunz, M., and Brown, I.D. (1995) Out-of-center distortions around octahedrally coordinated d<sup>0</sup> transition metals. *Journal of Solid State Chemistry*, 115, 395–406.
- Kunz, M., Leinenweber, K., Parise, J.B., Wu, T.C., Bassett, W.A., Brister, K., Weidner, D.J., Vaughan, M.T., Wang, Y. (1996) The baddeleyite-type high pressure phase of Ca(OH)<sub>2</sub>. *High Pressure Research*, 14, 311–319.
- Kunz, M., Xirouchakis, D., Wang, Y., Parise, J.B., and Lindsley, D.H. (1997) Structural investigation along the join CaSnOSiO<sub>4</sub>-CaTiOSiO<sub>4</sub>. *Schweizerische Mineralogische und Petrographische Mitteilungen*, in press.
- Larson, A.C., and Von Dreele, R.B. (1986) GSAS, General Structure Analysis System. Los Alamos National Laboratory, LAUR 86-748.
- LeBail, A. (1992) Extracting structure factors from powder diffraction data by iterating full pattern profile fitting. In E. Prince and J.K. Stalick, Eds., *Accuracy in powder diffraction II*, Special Publication 846, p. 213. National Institute of Standards and Technology, Gaithersburg, Maryland.
- Oberti, R., Smith, D.C., Rossi, G., and Caucia, F. (1991) The crystal chemistry of high-aluminum titanites. *European Journal of Mineralogy*, 3, 777–792.
- Speer, J.A., and Gibbs, G.V. (1976) The crystal structure of synthetic titanite, CaTiOSiO<sub>4</sub>, and the domain textures of natural titanites. *American Mineralogist*, 61, 238–247.
- Taylor, M., and Brown, G.E. (1976) High-temperature structural study of the  $P2_1/a \rightleftharpoons A2/a$  phase transition in synthetic titanite, CaTiSiO<sub>5</sub>. *American Mineralogist*, 61, 435–447.
- Thompson, P., Cox, D., and Hastings, J. (1987) Rietveld refinement of Debye-Scherrer synchrotron X-ray data from Al<sub>2</sub>O<sub>3</sub>. *Journal of Applied Crystallography*, 20, 79–83.
- Zhang, M., Salje, E., Bismayer, U., Unruh, H., Wruck, B., and Schmidt, C. (1995) Phase transition(s) in titanite CaTiSiO<sub>5</sub>: An infrared spectroscopy, dielectric response and heat capacity study. *Physics and Chemistry of Minerals*, 22, 41–49.

MANUSCRIPT RECEIVED AUGUST 5, 1996

MANUSCRIPT ACCEPTED NOVEMBER 5, 1996